ORIGINAL ARTICLE



Cholesterol side groups in Helical Poly(3-alkylesterfurans)

Manami Kawakami¹ · Payton Downey¹ · Linda Peteanu¹ · Stefan Bernhard¹ · Kevin J. T. Noonan D

Received: 6 August 2022 / Revised: 20 October 2022 / Accepted: 11 November 2022 / Published online: 21 December 2022 © The Society of Polymer Science, Japan 2022

Abstract

Poly(3-alkylesterfurans) fold into helical conformations due to a preference for adjacent furan repeat units in the polymer backbone to adopt a *syn* conformation in which the oxygen atoms of the furan rings are oriented in the same direction. In this contribution, a new chiral helical poly(3-alkylesterfuran) is reported in which a cholesterol group has been attached to the backbone to ensure excess single-handed helix chirality. This rigid side group promotes a folded conformation of the polymer in chloroform, as evidenced by ¹H NMR, absorption, and circular dichroism studies. This is unique among previously reported helical poly(3-alkylesterfurans) with *S*-3-octanol side chains, as those polymers are much more disordered in the same solvent. Circularly polarized luminescence studies also indicated how the chiroptical properties are impacted by intermolecular aggregation of these helical polymers. The study reveals the potential for tuning the properties of helical polyfurans via precise choice of the chiral side chain, which can be installed during monomer synthesis via a Steglich modification of 2-bromo-3-furoic acid. Suzuki-Miyaura cross-coupling polymerization produces the desired chiral helical polymers in reasonable yields with molecular weights above 10 kg/mol when the commercially available PEPPSI-IPent catalyst is used to catalyze cross-coupling.

Introduction

Combining semiconducting polymers and chiral side chains can offer access to redox-active materials that self-assemble into precise structures [1–5]. Noncovalent interactions such as π – π interactions or H-bonding lead to folding of single polymer chains into a helical conformation (right-handed or left-handed) or self-assembly of multiple chains into a chiral supramolecular assembly. A number of chiral conjugated polymers (CCPs) have been reported to date, including poly(phenylacetylenes) [6], oligo(m-phenylene ethynylene)s [7, 8], poly(3,6-carbazoles) [9], poly(3,6-phenanthrene)s [10], gallic acidfunctionalized poly(dithienopyrroles) [11] and polyfluorenes [12]. While many examples of CCPs are known, chiral polythiophenes have attracted significant attention

Supplementary information The online version contains supplementary material available at https://doi.org/10.1038/s41428-022-00741-w.

[13] since the properties of polythiophenes have been well studied [14], chain-growth polymerization makes it possible to synthesize well-defined polymers [15–18], and various functional groups can be attached as side chains through the 3-position of the thiophene ring. Gallic acid [19], sulfonyl [20] and sugar-based [21] polythiophenes all folded into helical structures, which was driven by the choice of the side chain.

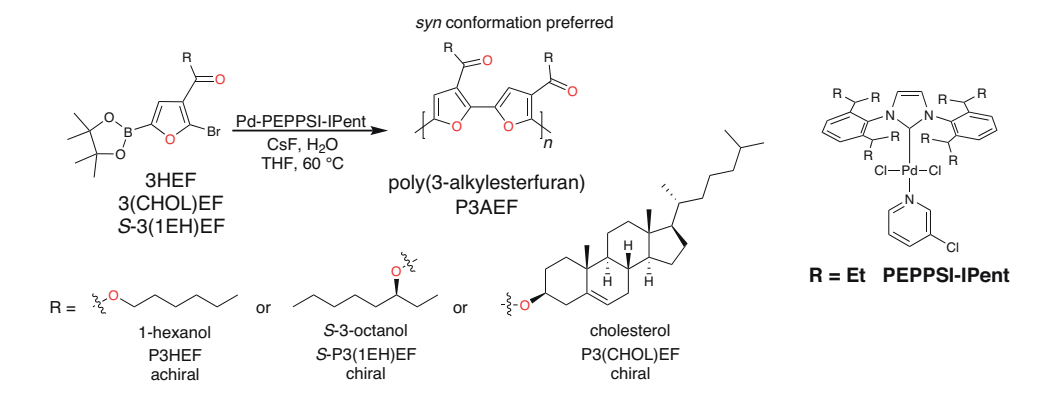
While chiral polythiophenes have been desirable synthetic targets, chiral polymers derived from other Group 16 heterocycles, such as furan, selenophene or tellurophene, are very rare. Polyfurans [22–24] have attracted attention as organic materials since they are typically more luminescent than the heavier polychalcogenophenes and can be sourced from biobased resources. In our own work, we noted that polyfurans with ester side chains spontaneously folded into compact π -stacked helical structures due to the preference for adjacent furan-3-carboxylates to adopt syn conformations (Fig. 1) [25]. To our knowledge, poly(3-hexylesterfuran) or P3HEF was the first example of a helical polyfuran, and attachment of a chiral side chain (S-3-octanol to form S-P3(1EH)EF) enabled the formation of a chiral helical polymer, as evidenced by circular dichroism studies in 60:40 MeOH:CHCl₃ [25]. Herein, we expand this methodology and use a derivative from the chiral pool to make a CCP. Specifically, we demonstrate that cholesterol,

 [⊠] Kevin J. T. Noonan noonan@andrew.cmu.edu

Department of Chemistry, Carnegie Mellon University, 4400 Fifth Avenue, Pittsburgh, PA 15213-2617, USA

566 M. Kawakami et al.

Fig. 1 Synthetic approach to chiral helical polyfurans. The two different chiral side chains for the poly(3-alkylesterfurans) (P3AEFs) are indicated with the monomer and polymer abbreviations noted



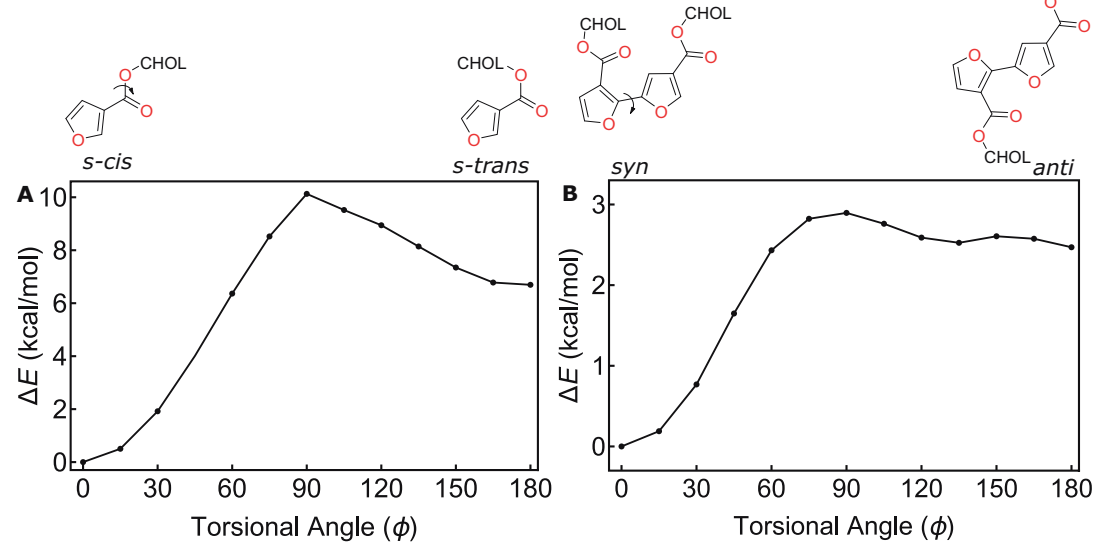


Fig. 2 Torsional potential energy scans calculated using semiempirical methods (PM6) for cholesterol furan 3-carboxylate (**A**) and cholesterol [2,2'-bifuran]-3,4'-dicarboxylate (**B**). For cholesterol furan 3-

carboxylate, the dihedral angle around the ester bond was constrained (OCOC), and in cholesterol [2,2'-bifuran]-3,4'-dicarboxylate, the dihedral angle around the interring bond was constrained (OCCO)

CHOL

a widely available chiral alcohol, can be appended to the polyfuran scaffold to afford a chiral helical polyfuran in a straightforward manner.

A regioregular, helical poly(3-cholesterolesterfuran) (P3(CHOL)EF) can be synthesized in good yield using Suzuki-Miyaura cross-coupling, as shown in Fig. 1 (M_n = 84.9 kg/mol, yield = 65%). A commercially available N-heterocyclic carbene palladium catalyst, namely, PEPPSI IPent, is very effective in polymerization of 3-alkylester furans and produces polymers with molecular weights >10 kg/mol (Fig. 1). We have noted that while an S-3octanol side chain disrupted formation of a compact helical P3AEF in chloroform, the cholesterol side group led to a highly ordered helical structure under the same conditions, as evidenced by ¹H NMR, absorption, and CD spectroscopy. Moreover, a significant dissymmetry factor ($g_{em} =$ 0.05) was noted for P3(CHOL)EF in n-octane at room temperature, which was likely due to the formation of larger polymer aggregates.

Results and discussion

Prior to the synthesis of P3(CHOL)EF, torsional potentials were computed to identify whether a syn or anti conformation would be favored for the furan rings, with the expectation that a syn preference would lead to a helical geometry in the final polymer. A torsional scan around the ester bond for cholesterol furan-3-carboxylate was performed first (Fig. 2A) to determine the lowest energy conformer for the relatively bulky ester side chain. The dihedral angle around the ester bond was constrained at 15° intervals from 0° (s-cis) to 180° (s-trans), and each conformer was optimized with semiempirical methods. The s-cis conformation was identified as the low-energy rotamer and was favored over the *s-trans* conformation by 6.7 kcal/mol. This is consistent with observations for other unsaturated esters, such as methyl acrylate and acrylic acid [26]. The side chain conformation was then used as a starting point to build the cholesterol-functionalized [2,2'-bifuran]-3,4'-dicarboxylate to gain insight into the conformational preferences of the polymer. The interring bond was constrained at 15° intervals from 0° (*syn*) to 180° (*anti*), as shown in Fig. 2B [27–29]. Again, the optimizations were carried out using semiempirical methods to reduce the computational cost, and the *syn* conformer emerged as the global minimum, as expected from prior work [25]. The *syn* conformation was more stable than the *anti* conformer by nearly 2.5 kcal/mol, and the rotational barrier was ~2.9 kcal/mol. Altogether, the computational results suggested that the s-*cis* conformation is preferred for the side chain and that adjacent furan cholesterol furan 3-carboxylates will adopt the necessary *syn* configuration to give a helical geometry.

Once the computational analysis was complete, P3(CHOL)EF was synthesized using Suzuki-Miyaura crosscoupling polymerization (Fig. 1). The cholesterol furan-3carboxylate monomer was prepared starting from furan-3carboxylic acid. The three-step synthetic sequence is outlined in detail in Scheme S1, and experimental details for monomer preparation can be found in the Supporting Information. Briefly, 2-bromofuran-3-carboxylic acid was obtained by metalation of furan-3-carboxylic acid with two equivalents of *n*-butyllithium, followed by electrophilic quenching with Br₂ [25]. Steglich esterification was then accomplished with cholesterol in dichloromethane (27% yield). Finally, the pinacol boronic ester group was installed at the 5-position of the furan by using iridium-catalyzed borylation [30] to give the desired 3-cholesterolesterfuran (3(CHOL)EF) in 81% yield.

Then, PEPPSI-IPent was used to bring about polymerization of the 3(CHOL)EF monomer, as well as our previously synthesized S-3(1EH)EF monomer (Fig. 1) [25]. The PEPPSI catalyst systems have been specifically designed to promote the most challenging cross-coupling reactions [31], and we have noted that the commercially available PEPPSI-IPent is exceptionally effective for polymerization of ester-functionalized thiophenes and selenophenes [32]. Polymerizations of 3(CHOL)EF and S-3(1EH) EF were carried out at 60 °C in a 5:1 THF:H₂O mixture. In both instances, 3 mol% of the PEPPSI-IPent catalyst was used, and 3 equivalents of CsF were employed as the inorganic base to promote cross-coupling. During the polymerization of S-3(1EH)EF, a change from a red to dark red solution was observed, whereas polymerization of 3(CHOL)EF resulted in a persistent brown color. Both polymerizations were quenched with 6 M HCl/MeOH after 1 h, and yields of 81 and 65% were obtained for S-P3(1EH) EF and P3(CHOL)EF, respectively. The as-obtained polymers were then washed with hot acetone and reprecipitated by methanol to remove additional impurities. A single monomodal peak was noted in the GPC traces for both polymers when carried out with 10 mM LiNTf₂/THF as the eluent, but the molecular weight estimate for P3(CHOL)EF

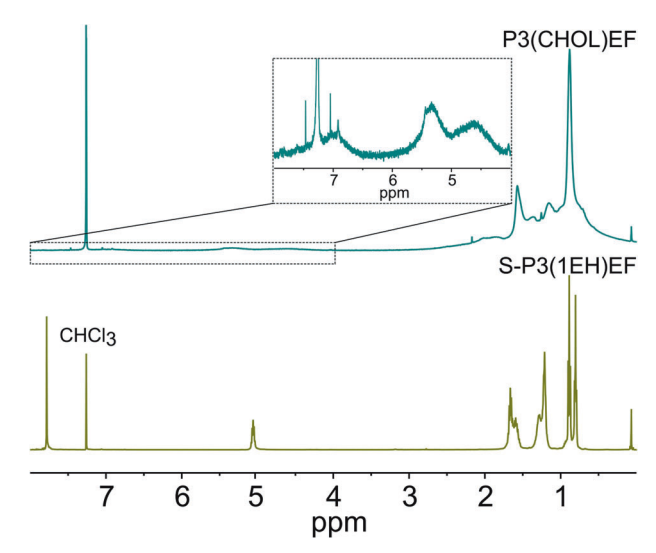


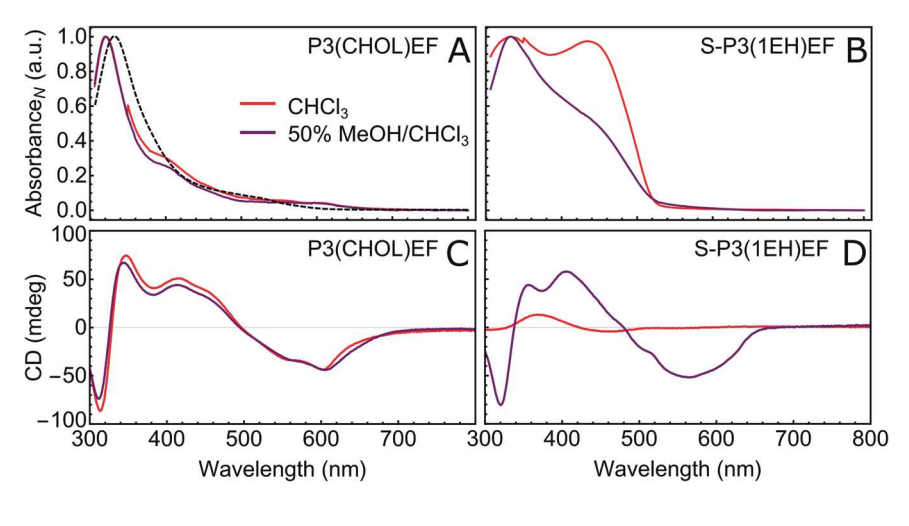
Fig. 3 1 H NMR spectra (500 MHz) of P3(CHOL)EF (M_n = 84.9 kg/mol) and S-P3(1EH)EF (M_n = 14.1 kg/mol) acquired at 25 $^{\circ}$ C in CDCl₃

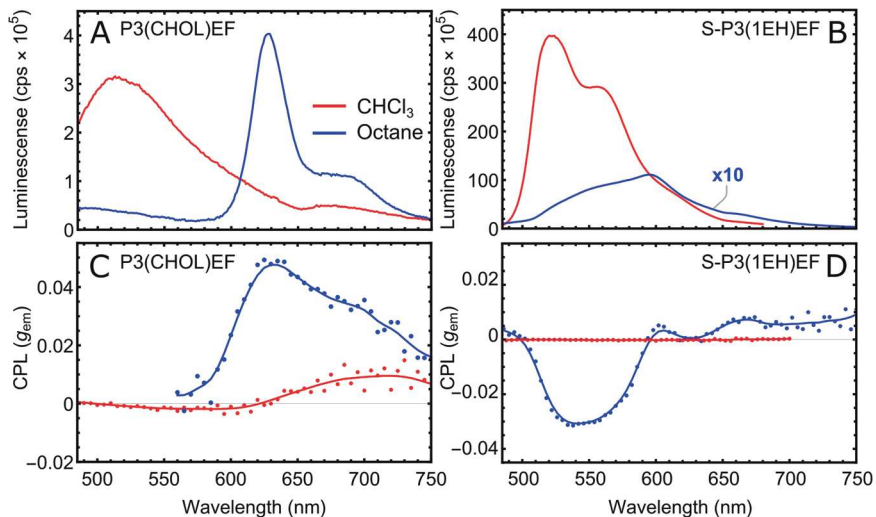
 $(M_{\rm n}=84.9~{\rm kg/mol},~D=2.0)$ was much higher than that of S-P3(1EH)EF ($M_{\rm n}=14.1~{\rm kg/mol},~D=1.3$). While it is not surprising that the cholesterol-functionalized polymer had a higher molar mass given the larger molecular weight of the repeat unit, the difference between the two polymers was quite high. It is possible that the cholesterol side chain led to more intermolecular aggregation between polymer chains, which could result in overestimation of the molecular weight for P3(CHOL)EF. We have noted that addition of LiNTf2 into the THF eluent resulted in a narrower, more symmetrical peak in the GPC analysis of P3(CHOL)EF, while the added salt had minimal impact on the GPC profile for S-P3(1EH)EF.

The ¹H NMR spectrum for P3(CHOL)EF in CDCl₃ provided strong evidence that the cholesterol resulted in a compact folded configuration for the polyfuran (Fig. 3). The signals in the ¹H NMR spectrum for P3(CHOL)EF were broad, as the aromatic and vinyl signals spanned nearly 770 and 480 Hz, respectively (Fig. 3—top). The broad ¹H NMR signals were a result of restricted chain motion, which led to magnetically inequivalent protons along the chain [25]. The broadening of the spectrum did not change upon heating P3(CHOL)EF to 80 °C in 1,1,2,2-tetrachloroethane- d_2 , suggesting that the folded structure was retained upon mild heating in a chlorinated solvent. These results were in sharp contrast to the ¹H NMR spectrum of S-P3(1EH)EF in CDCl₃ at room temperature, where a sharp aromatic signal with a width of only 25 Hz was observed (Fig. 3—bottom). The conformational differences between P3(CHOL)EF and S-P3(1EH)EF likely led to the differences observed in the ¹H NMR spectra shown in Fig. 3. The sharp signals noted for S-P3(1EH)EF suggested that protons along the backbone were chemically equivalent and that chain motion of 568 M. Kawakami et al.

Fig. 4 UV-vis absorption (A and B) and circular dichroism spectra (C and D) of 0.03 mg/ mL solutions of P3(CHOL)EF $(M_n = 84.9 \text{ kg/mol})$ and S-P3(1EH)EF $(M_n = 14.1 \text{ kg/mol})$. The red plots correspond to spectra collected in 100% CHCl₃, and the purple plots correspond to spectra collected in 1:1 CHCl₃:CH₃OH. The black dotted line in (A) corresponds to the absorption spectrum of P3HEF ($M_n = 6.9 \text{ kg/mol}$) collected in CHCl₃ (0.03 mg/ mL)

Fig. 5 Luminescence spectra (A and B) and circularly polarized luminescence dissymmetries (g_{em}) (C and D) of P3(CHOL)EF ($M_n = 84.9 \text{ kg/}$ mol) and S-P3(1EH)EF $(M_n = 14.1 \text{ kg/mol})$ measured in chloroform (red) and n-octane (blue) (0.06 mg/mL). P3(CHOL) EF was excited at 400 nm, and S-P3(1EH)EF was excited at 450 nm. The luminescence spectrum of S-P3(1EH)EF in octane is enlarged by a factor of 10 to better show the spectral shape. Raw CPL data were fit with Gaussian functions to add a trendline





the polymer was not restricted in this solvent at room temperature, so the polymer was more disordered or unfolded. These signals broaden upon addition of a non-solvent (MeOH), demonstrating that a more folded conformation with S-P3(1EH)EF was possible under appropriate conditions [25]. While folding in S-P3(1EH)EF can be controlled via solvent mixtures, the rigid cholesterol side chain ensured that the polyfuran retained a compact helical structure, even when dissolved in a good solvent such as CHCl₃.

The UV–vis and CD spectra collected for P3(CHOL)EF and S-P3(1EH)EF also provided strong evidence that the side chain played a significant role in folding of polyfurans into compact helical conformations. Helical polyfurans should produce a λ_{max} near 330 nm, with tailing into the visible region, as discussed in the prior report on P3HEF [25]. This unique spectral signature arises from partial cancellation of the transition dipole vectors when summed along the circular path of the polymer, as the low energy π - π * transition has a very low oscillator strength in this conformation [25]. The absorption spectrum for P3(CHOL)

EF in CHCl₃ matched almost exactly with the absorption spectrum collected for P3HEF (red and black trace in Fig. 4A). A strong chiroptical response was noted for P3(CHOL)EF, with a bisignate Cotton effect for the high energy transition at 330 nm, a positive Cotton effect for the transition near ~410 nm and a negative Cotton effect for the transition at ~610 nm (Fig. 4C—red trace). Together, the CD and UV–Vis spectra for P3(CHOL)EF provided strong evidence that the polymer adopted a helical conformation [25].

In contrast, the absorption spectrum of *S*-P3(1EH)EF collected in CHCl₃ was quite different from that of P3(CHOL)EF, with two major bands of nearly equal intensity at 330 and 435 nm (Fig. 4B—red trace). The strength of the low energy transition at 435 nm in the absorption spectrum and the low ellipticity noted for the signals in the CD spectrum of *S*-P3(1EH)EF in CHCl₃ indicated that the polymer was partially unfolded in this solvent (Fig. 4D—red trace) [25]. Addition of a nonsolvent (MeOH) led to a decrease in the intensity of the 435 nm band in the absorption spectrum (purple trace in Fig. 4B)

and an increase in the CD signal intensity (Fig. 4D—purple trace). This suggested a transition from the partially unfolded state in a good solvent to a more compact folded conformation upon addition of a nonsolvent. No change was noted in the absorption or CD spectra of P3(CHOL)EF in 1:1 CHCl₃:MeOH, suggesting that the nonsolvent had no effect on the polymer with the cholesterol side chain. The CD spectra for both polymers were similar, with a bisignate signal near 320 nm, followed by positive and negative Cotton effects at longer wavelengths, consistent with them having the same helix handedness.

The CPL spectra of P3(CHOL)EF and S-P3(1EH)EF were measured to gain further insights into the properties of these two chiral polymers. Interestingly, changes in the solvent environment caused substantial differences in the luminescence spectra and the chiroptical responses for the materials. While both were luminescent in CHCl3 (red traces in Fig. 5A and B), dissymmetry factors of $\sim 10^{-3}$ were noted for both polymers (red traces in Fig. 5C and D), which were within expectations for polymeric π -systems [33]. Of note, the luminescence intensity observed for P3(CHOL)EF was 100× lower than that for S-P3(1EH)EF in CHCl₃, suggesting stronger intrachain interactions in the cholesterol material, consistent with the conclusions from NMR, UV-Vis and CD data. This intrachain aggregation caused increased fluorescence quenching, and thus, this material was markedly less emissive than S-P3(1EH)EF. While the insights regarding chain folding were helpful, the small g_{em} values led to a search for solvents that could dissolve these polyfurans and also result in higher chiroptical responses. Addition of a nonsolvent was used to alter the response, but the CPL measurement for P3(CHOL) EF was not markedly different when performed in CHCl₃ or in 1:1 CHCl3:MeOH (Fig. S11). It was also difficult to dissolve these polyfurans in 1:1 CHCl₃:MeOH at 0.06 mg/ mL concentrations, which limited the mixed solvent approach in this case.

Nonpolar solvents such as hexane or octane were also considered, since polyfurans are quite soluble in a wide range of nonpolar solvents. This resulted in large bathochromic shifts for the emission maxima of P3(CHOL)EF and S-P3(1EH)EF when compared to the luminescence spectra recorded in CHCl₃ (100 and 60 nm, respectively). A small increase in the luminescence intensity was noted for P3(CHOL)EF on going from CHCl₃ to octane, while the S-P3(1EH)EF emission was dramatically reduced in octane (blue traces in Fig. 5A and B). The observed redshift clearly indicated that the octane solvent environment led to increased chromophore-chromophore interactions, and the CPL data provided further evidence for this claim. Both P3(CHOL)EF and S-P3(1EH)EF exhibited unusually large emission dissymmetries in octane when compared to the corresponding CHCl₃ data. The S-P3(1EH)EF polymer exhibited bisignate CPL characteristics, a phenomenon that is not unusual for aggregating polymeric π -systems [33]. The more rigid cholesterol-based polyfuran had a uniform CPL response similar to that expected for simpler/molecular luminophores. The $g_{\rm em}$ observed for this polymer reached 0.05, which hinted at an increased size for the polymeric aggregates and a stronger long-range association holding the ensembles together.

Dynamic light scattering (DLS) measurements provided strong evidence for aggregation in nonpolar solvents, although no visible precipitation was noted for either polymer in *n*-octane at 0.06 mg/mL. The number-weighted size distributions measured for P3(CHOL)EF and S-P3(1EH)EF in CHCl₃ at room temperature were 6.8 ± 0.8 and 6.7 ± 0.5 nm, respectively (Fig. S6). In contrast, the number weighted distributions were markedly larger in noctane, suggesting significant aggregation. The size distribution measured for P3(CHOL)EF in n-octane at room temperature was 634.9 ± 21.1 nm, whereas for S-P3(1EH) EF, it was 26.1 ± 2.1 nm. The large difference in the size of the polymer aggregates was likely related to the exceptional self-assembly properties of cholesterol molecules, which enhanced intermolecular interactions between P3(CHOL) EF chains. Aggregation of both polymers in *n*-octane led to subtle differences in the CD spectra, as shown in the Supporting Information (Figs. S9–S10).

In conclusion, we have successfully synthesized a poly(3-alkylesterfuran) derivative with a pendant cholesterol side chain. The rigid cholesterol group facilitated formation of a chiral helical polymer with a compact folded conformation, as evidenced by ¹H NMR, UV-Vis, and CD spectroscopic studies. Comparison of ester-functionalized polyfurans bearing either a cholesterol or S-3-octanol side chain revealed how chain folding in these systems was impacted by the choice of chiral side group. In addition, CPL and DLS studies illustrated how chiroptical properties changed as a function of intermolecular aggregation by the polyfurans. Clearly, the optical activities, luminescence and chain folding of these polymers are tunable, either with the choice of side chain or solvent. In future work, we will examine how other enantiopure building blocks derived from natural resources can be used to alter the chiroptical properties of helical polyfurans. More in-depth examination of the electronic structure will be used to better understand the unique absorption and CD spectra noted for these macromolecules.

Acknowledgements KJTN and SB are grateful to the NSF for support of this work (CHE-2109065 and CHE-2102460).

Compliance with ethical standards

Conflict of interest The authors declare no competing interests.

570 M. Kawakami et al.

References

- Yashima E, Ousaka N, Taura D, Shimomura K, Ikai T, Maeda K. Supramolecular Helical Systems: Helical Assemblies of Small Molecules, Foldamers, and Polymers with Chiral Amplification and Their Functions. Chem Rev. 2016;116:13752–990.
- Yashima E, Maeda K, Iida H, Furusho Y, Nagai K. Helical Polymers: Synthesis, Structures, and Functions. Chem Rev. 2009;109:6102–211.
- Nakano T, Okamoto Y. Synthetic Helical Polymers: Conformation and Function. Chem Rev. 2001;101:4013–38.
- Verswyvel M, Koeckelberghs G. Chirality in Conjugated Polymers: When Two Components Meet. Polym Chem. 2012;3:3203–16.
- Kane-Maguire LAP, Wallace GG. Chiral Conducting Polymers. Chem Soc Rev. 2010;39:2545

 –76.
- Freire F, Quiñoá E, Riguera R. Supramolecular Assemblies from Poly(phenylacetylene)s. Chem Rev. 2016;116:1242–71.
- 7. Brunsveld L, Prince RB, Meijer EW, Moore JS. Conformational Ordering of Apolar, Chiral *m*-Phenylene Ethynylene Oligomers. Org Lett. 2001;2:1525–8.
- 8. Brunsveld L, Meijer EW, Prince RB, Moore JS. Self-Assembly of Folded *m*-Phenylene Ethynylene Oligomers into Helical Columns. J Am Chem Soc. 2001;123:7978–84.
- Hu Y, Song F, Xu Z, Tu Y, Zhang H, Cheng Q, et al. Circularly Polarized Luminescence from Chiral Conjugated Poly(carbazoleran-acridine)s with Aggregation-Induced Emission and Delayed Fluorescence. ACS Appl Polym Mater. 2019;1:221–9.
- Vanormelingen W, Smeets A, Franz E, Asselberghs I, Clays K, Verbiest T, et al. Conformational Steering in Substituted Poly(3,6phenanthrene)s: A Linear and Nonlinear Optical Study. Macromolecules 2009;42:4282–7.
- Vanormelingen W, Van den Bergh K, Verbiest T, Koeckelberghs G. Conformational Transitions in Chiral, Gallic Acid-Functionalized Poly(dithienopyrrole): A Comparative UV-vis and CD Study. Macromolecules 2008;41:5582–9.
- Wang Y, Harada T, Phuong LQ, Kanemitsu Y, Nakano T. Helix Induction to Polyfluorenes Using Circularly Polarized Light: Chirality Amplification, Phase-Selective Induction, and Anisotropic Emission. Macromolecules 2018;51:6865–77.
- Wang K, Xiao Y. Chirality in Polythiophenes: A Review. Chirality 2021;33:424

 –46.
- 14. Ewbank PC, Stefan MC, Sauvé G, McCullough RD. Synthesis, Characterization and Properties of Regioregular Polythiophene-Based Materials. In Handbook of Thiophene-Based Materials. In: Perepichka, IF;, Perepichka DF, editors. Chichester, UK: John Wiley & Sons, Ltd; 2009. p. 157–217.
- McCullough RD, Lowe RD. Enhanced Electrical Conductivity in Regioselectively Synthesized Poly(3-alkylthiophenes). J Chem Soc Chem Commun. 1992;70–2.
- Miyakoshi R, Yokoyama A, Yokozawa T. Synthesis of Poly(3-hexylthiophene) with a Narrower Polydispersity. Macromol Rapid Commun. 2004;25:1663–6.
- Sheina EE, Liu J, Iovu MC, Laird DW, McCullough RD. Chain Growth Mechanism for Regioregular Nickel-Initiated Cross-Coupling Polymerizations. Macromolecules 2004;37:3526–8.
- Yokoyama A, Miyakoshi R, Yokozawa T. Chain-Growth Polymerization for Poly(3-hexylthiophene) with a Defined Molecular Weight and a Low Polydispersity. Macromolecules 2004;37:1169–71.

Leysen P, Teyssandier J, De Feyter S, Koeckelberghs G. Controlled Synthesis of a Helical Conjugated Polythiophene. Macromolecules 2018;51:3504

–14.

- Wang P, Jeon I, Lin Z, Peeks MD, Savagatrup S, Kooi SE, et al. Insights into Magneto-Optics of Helical Conjugated Polymers. J Am Chem Soc. 2018;140:6501–8.
- Ikai T, Takayama K, Wada Y, Minami S, Apiboon C, Shinohara K. Synthesis of a One-Handed Helical Polythiophene: A New Approach Using an Axially Chiral Bithiophene with a Fixed synconformation. Chem Sci. 2019;10:4890–5.
- Gidron O, Dadvand A, Wei-Hsin Sun E, Chung I, Shimon LJW, Bendikov M, et al. Oligofuran-Containing Molecules for Organic Electronics. J Mater Chem C. 2013;1:4358–67.
- Gidron O, Bendikov M. α-Oligofurans: An Emerging Class of Conjugated Oligomers for Organic Electronics. Angew Chem Int Ed. 2014;53:2546–55.
- Jin X-H, Sheberla D, Shimon LJW, Bendikov M. Highly Coplanar Very Long Oligo(alkylfuran)s: A Conjugated System with Specific Head-To-Head Defect. J Am Chem Soc. 2014;136:2592–601.
- Varni AJ, Fortney A, Baker MA, Worch JC, Qiu Y, Yaron D, et al. Photostable Helical Polyfurans. J Am Chem Soc. 2019;141:8858–67.
- Jones GIL, Owen NL. Molecular Structure and Conformation of Carboxylic Esters. J Mol Struct. 1973;18:1–32.
- Bloom JWG, Wheeler SE. Benchmark Torsional Potentials of Building Blocks for Conjugated Materials: Bifuran, Bithiophene, and Biselenophene. J Chem Theory Comput. 2014;10:3647–55.
- Lin JB, Jin Y, Lopez SA, Druckerman N, Wheeler SE, Houk KN. Torsional Barriers to Rotation and Planarization in Heterocyclic Oligomers of Value in Organic Electronics. J Chem Theory Comput. 2017;13:5624–38.
- Topolskaia V, Pollit AA, Cheng S, Seferos DS. Trends in Conjugated Chalcogenophenes: A Theoretical Study. Chem Eur J. 2021;27:9038–43.
- Chotana GA, Kallepalli VA, Maleczka RE, Smith MR. Iridium-Catalyzed Borylation of Thiophenes: Versatile, Synthetic Elaboration Founded on Selective C-H Functionalization. Tetrahedron 2008;64:6103–14.
- Valente C, Çalimsiz S, Hoi KH, Mallik D, Sayah M, Organ MG. The Development of Bulky Palladium NHC Complexes for the Most-Challenging Cross-Coupling Reactions. Angew Chem Int Ed. 2012;51:3314–32.
- 32. Kawakami M, Schulz KHG, Varni AJ, Tormena CF, Gil RR, Noonan KJT. Statistical Copolymers of Thiophene-3-carboxylates and Selenophene-3-carboxylates; ⁷⁷Se NMR as a Tool to Examine Copolymer Sequence in Selenophene-based Conjugated Polymers. Polym Chem. 2022;13:5316–24.
- 33. Duong ST, Fujiki M. The Origin of Bisignate Circularly Polarized Luminescence (CPL) Spectra from Chiral Polymer Aggregates and Molecular Camphor: anti-Kasha's Rule Revealed by CPL Excitation (CPLE) Spectra. Polym Chem. 2017;8:4673–9.

Publisher's note Springer Nature remains neutral with regard to jurisdictional claims in published maps and institutional affiliations.

Springer Nature or its licensor (e.g. a society or other partner) holds exclusive rights to this article under a publishing agreement with the author(s) or other rightsholder(s); author self-archiving of the accepted manuscript version of this article is solely governed by the terms of such publishing agreement and applicable law.